The location and annealing of paramagnetic oxygen vacancies (E_1' centres) in silicon implanted with high doses of oxygen

The location and annealing of paramagnetic oxygen vacancies (E'$_1$ centres) in silicon implanted with high doses of oxygen

R C Barklie†, T J Ennis†, K Reeson‡ and P L F Hemment‡

† Physics Department, Trinity College, Dublin 2, Ireland
‡ Electronic and Electrical Engineering Department, University of Surrey, Guildford, Surrey, UK

Abstract. Electron paramagnetic resonance measurements have been made on samples of (100) n-type silicon which have been implanted with 200 keV oxygen ions in the implantation temperature range of 500–620 °C and with doses ranging from 0.5 to 2.2×10^{18} O cm^{-2}. Amongst the various defects observed in the as-implanted samples are E'$_1$ centres whose population per unit area of implanted surface exhibits a maximum at a dose of 1.4×10^{18} cm^{-2}, which is the dose above which a continuous buried oxide layer is formed. These E'$_1$ centres, in a sample implanted with 1.8×10^{18} O cm^{-2}, begin to anneal at about 350 °C—a process which is irreversible. Subsequent electron or γ-irradiation at room temperature increases the E'$_1$ centre concentration but only in those samples containing a buried oxide layer. This increase saturates at a dose of about 7 Mrad. The results can be explained by assuming that for the as implanted samples all E'$_1$ centres are in the oxide precipitates and that those 're-activated' by electron or γ irradiation are all in the buried layer. The latter also begin to anneal irreversibly at about 350 °C but can be annealed reversibly at lower temperatures. The anneal mechanisms are examined in the light of these results.

1. Introduction

E'$_1$ centres, which are singly ionized oxygen vacancies $\equiv$ Si$^+ \cdot$ Si $\equiv$, are one of the commonest type of defects in all forms of SiO$_2$ [1]. They have added importance because the trapped positive charge in the oxide of MOS and related electronic devices is largely due to these defects [2]. Despite intensive study their anneal mechanisms remain uncertain. In this paper we compare the anneal behaviour of E'$_1$ centres in oxide precipitates and in continuous oxide layers in silicon and from this draw conclusions about the nature of those mechanisms.

The samples were prepared by implanting silicon wafers with very large doses ($\approx 10^{18}$ O cm^{-2}) of oxygen ions—in some cases sufficiently large to form an oxide layer buried beneath the silicon surface—and to keep the silicon crystalline this was done at an implantation temperature of about 500–600 °C. Because the dose is so high the samples in the as-implanted state contain many oxide precipitates, as well as a buried oxide layer, and so provide a unique opportunity for comparing the behaviour of E'$_1$ centres in these two regions. The main purpose of this (SIMOX) process is to provide high quality silicon-on-insulator material and to this end it is subsequently

necessary to anneal the material at a temperature of about $1300\,^{\circ}C$, but this was not done in the present case.

Our experiments were in fact begun with the aim of determining the location of the E_1' centres. Some earlier measurements [3] suggested that the E_1' centres are in the buried layer but this conclusion appeared to be contradicted by later experiments which showed that there certainly are E_1' centres in the precipitates [4]. We started therefore with the aim of determining whether these centres are in both regions or only in one. The results presented in sections 4.1 and 4.2 provide strong evidence that the as-implanted samples contain E_1' centres only in the precipitates but that E_1' precursors remain in the buried layer which can be converted to E' centres by electron or γ irradiation. Section 4.3 presents the anneal data which as well as providing additional evidence for our hypothesis also allow a comparison to be made of the annealing behaviour of the E_1' centres in these two locations. In section 5 we discuss which of the many variants of E' centre exists in our samples. Section 6 discusses the possible anneal mechanisms in the light of the results presented earlier.

2. Sample preparation and structure

All samples were prepared at the University of Surrey by implanting device grade n-type (100) silicon wafers with either 200 keV $^{16}O^+$ or 400 keV $^{32}O_2^+$; the latter dissociate on impact and so only the equivalent O^+ dose is given. The samples studied had doses of 0.5, 0.75, 0.8, 0.95, 1.2, 1.4, 1.8 (using $^{32}O_2^+$), 1.8 (using $^{16}O^+$) and 2.2×10^{18} O cm^{-2} at an implantation temperature of 540, 570, 580, 580, 620, 600, 520, 560 and 500 $^{\circ}C$ respectively. The samples were mounted on silicon tips to reduce heat loss by conduction and were heated solely by the ion beam.

The structure of some or all of these samples has been studied using cross-section transmission electron microscopy (TEM) [5, 6], secondary ion mass spectrometry (SIMS) [7, 8], Rutherford backscattering [6, 8], infrared absorption and Raman scattering [9] and we now briefly summarize those features of relevance to the present study. TEM shows that, in the as-implanted state, only the samples with doses of (1.8 and 2.2) $\times 10^{18}$ cm^{-2} have a *continuous* buried amorphous layer with thickness of about 0.28 and 0.41 μm respectively. This layer is shown by SIMS to be stoichiometric SiO$_2$. For a dose of 1.4×10^{18} O cm^{-2} the peak oxygen concentration very nearly reaches that for bulk SiO$_2$ so that this dose may be regarded as having the critical value, ϕ_c, above which a continuous layer of SiO$_2$ is formed in the as-implanted state.

All samples contain oxide precipitates. Infrared absorption shows that, at least for the sample with a dose of 1.4×10^{18} O cm^{-2}, these are under compressive stress and that some have a sub-oxide composition, i.e. SiO$_x$, $x < 2$. No details are available of the size of these precipitates in our samples but measurements [10–13] made on similar ones show them mostly to be less than or equal to 10 nm in diameter and show that as the oxygen concentration increases with depth so too does the average size of the precipitates and that the largest ones occur either at the peak of the oxygen distribution if no buried layer is present or, if it is, adjacent to this layer.

3. Technical details

Electron paramagnetic resonance (EPR) measurements were made at Trinity College at room temperature, at a microwave frequency of about 9.6 GHz, and with 100 kHz field modulation.

Additional sample irradiations were done at room temperature with either 30 keV electrons in a SEM or 0.662 MeV γ-rays from a ^{137}Cs source. A Faraday cup was used to monitor the electron beam current impinging on the sample; this current was typically 0.3 nA.

4. Results

4.1. The as-implanted state

We consider first the results obtained before any additional irradiations or anneals. Figure 1 shows the EPR spectrum of a sample implanted with a dose of 1.8×10^{18} O cm^{-2}. The two features A and C are common to all the samples except one: feature C is undetectable for the lowest dose sample. The defects (amorphous silicon centres in bulk silicon and P_b centres at oxide precipitate/silicon interfaces; P_b centres are silicon dangling bonds at Si/SiO$_2$ interfaces) which are responsible for feature A have been discussed elsewhere [3]. Here we are concerned only with the feature C. It is slightly asymmetric, isotropic, has a zero crossing g value, g_0, (corresponding to the point where the signal crosses the base line) of 2.0003 ± 0.0004, saturates easily with increasing microwave power and, for a dose of 1.4×10^{18} O cm^{-2}, has a peak-to-peak linewidth of 0.30 ± 0.03 mT. These characteristics are similar to those of E_1' centres produced in a-SiO$_2$ by ion implantation [14] and for this and other reasons given in section 5 we believe that feature C is due to these centres.
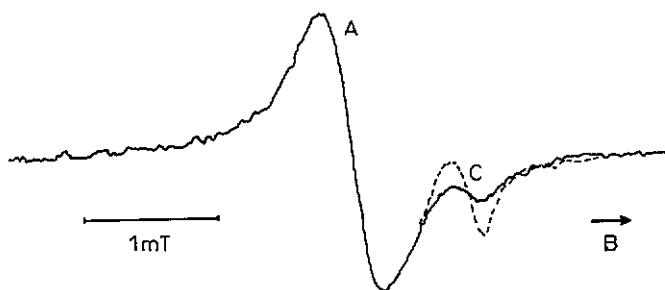

Figure 1. The EPR spectrum of the sample implanted with 1.8×10^{18} O cm^{-2} before (full line) and after (broken line) a 7 Mrad dose of 30 keV electrons. Magnetic field $\boldsymbol{B} \parallel$ [100]. Feature C is due to E$'$ centres.

We now consider those results of relevance to determining the location of the E_1' centres. When a sample implanted with 1.8×10^{18} O cm^{-2} was immersed in a KOH etch (for silicon) we found [3] that initially there was a decrease in the population of the amorphous silicon centres and P_b centres but no change in that of E_1' centres. This is certainly consistent with our original suggestion [3] that the latter are in the buried oxide layer. However, figure 2 shows that all samples, except that at the lowest dose of 0.5×10^{18} cm^{-2} in which the E_1' concentration was below the minimum detectable level of about 2×10^{12} cm^{-2}, contain E_1' centres including those samples *without* a buried layer. This implies that, whether or not they occur in the buried layer, the E_1' centres certainly exist in the oxide precipitates—at least for a dose $\phi < \phi_c$. The spin population was obtained by comparison of the spectrum intensity with that of a standard sample, from Varian, of pitch in KCL which consists of small particles
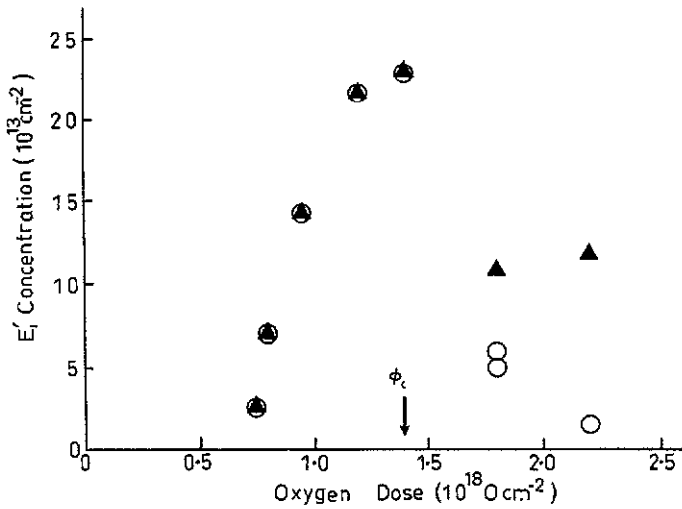
Figure 2. Dose dependence of the E' centre areal concentration before (open circle) and after (full triangles) irradiation with a 7 Mrad dose of 30 keV electrons. ϕ_c is the critical oxygen dose (1.4×10^{18} O cm^{-2}) above which a continuous buried oxide layer is formed.

of pitch uniformly distributed in KCL powder; relative values are correct to within about 10% but the absolute values may be in error by about a factor of two. The g_0 value shows no dependence on dose but the peak-to-peak linewidth does decrease smoothly from 0.43 ± 0.04 to 0.27 ± 0.04 mT as the dose is increased from 0.8 to 2.2×10^{18} cm^{-2} but, as figure 2 shows, it is the E_1' areal concentration $N(E_1')$ (i.e. the total population per unit area of implanted surface) which depends most strongly on dose. In view of the fact that, for the room temperature implantation of 30 keV O^+ into a-SiO_2, a maximum E_1' areal concentration is reached at a dose of about 5×10^{13} O cm^{-2} [15] it might be thought surprising that any increase in the $N(E_1')$ is seen at all in the 10^{18} O^+ cm^{-2} dose region. However, at these very high doses the O^+ ions are creating not only E_1' centres but also the material in which these centres occur. It is reasonable to suppose therefore that the increase in $N(E_1')$ with dose in the range $\phi < \phi_c$ is due, at least in part, to the increase in the total volume of precipitates per unit area of implanted surface. What is surprising is that as the dose is increased above ϕ_c the E_1' areal concentration falls even though the total volume of SiO_2 continues to increase. Although the areal concentration of E_1' centres, created by room temperature ion implantation into a-SiO_2, usually saturates at a high enough dose [14, 16] it was found that in the case of O^+ implantation it starts to decrease as the dose is increased above about 5×10^{13} O cm^{-2} and this was interpreted in terms of a dose-dependent self-annealing cross section [15]. In our case we believe that the decrease has another cause. It can hardly be coincidental that the decrease in $N(E_1')$ sets in when the dose exceeds that required for a continuous buried layer to form. This suggests that perhaps *all* the E_1' centres in *all* the samples occur only in the oxide precipitates so that when ϕ exceeds ϕ_c $N(E_1')$ starts to fall because a reduction occurs in the total volume of precipitates as they are incorporated into the buried layer. This raises the question of why no E_1' centres are present in the buried a-SiO_2 layer. This may be because the implantation temperature of 500–600 °C is well above that of about 100 °C at which E_1' centres, produced in a-SiO_2 by the room temperature

implantation of oxygen ions [15] and other ions [17], begin to anneal. However, it has been shown [15, 18] that, provided the anneal temperature does not exceed about 500 °C, this annealing process is reversible in the sense that the E_1' centres can be regenerated by small doses of ionizing radiation. It occurred to us therefore that such doses of radiation might regenerate E_1' centres in the buried a-SiO$_2$ layer.

4.2. Effects of ionizing radiation

Samples implanted with 1.8×10^{18} O$^+$ cm^{-2}, which contain a buried a-SiO$_2$ layer, were irradiated at room temperature with either 30 keV electrons in a SEM or 0.662 MeV γ-rays from a ^{137}Cs source. The time lapse between EPR measurements, reported here and in sections 4.3.2, and 4.3.3, which were made after electron irradiation and the irradiation itself was about 30 min. Both electron and γ-irradiations have the same effect which, as shown in figure 1, is to increase the intensity of feature C while feature A remains unchanged. Furthermore, since this is the only way in which feature C changes we conclude that the E' centres being regenerated are probably of the same type as the ones, which we have suggested are E_1' centres, that already exist. Moreover, as shown by Pfeffer [19], irradiation with 30 keV electrons, as well as transforming precursors, creates E_1' centres by radiolysis and 0.662 MeV γ-radiation will, in addition to these two processes, create them by atomic displacements produced by high-energy Compton electrons [20]. To check that the new E_1' centres arise from the conversion of precursors rather than by the other mechanisms we measured the E_1' population as a function of both γ-ray and electron dose for a sample with $\phi = 1.8 \times 10^{18}$ O$^+$ cm^{-2}. We find that it does increase initially but that the *additional* E_1' areal concentration saturates at a value of 5.8×10^{13} cm^{-2} at an absorbed dose of about 5 Mrad for γ-rays or about 7 Mrad for electrons. The electron dose was calculated using the value of 1850 eV for the energy deposited by each 30 keV electron in traversing a 500 nm SiO$_2$ film [19]. There are two reasons for believing that this behaviour implies that the creation mechanism is the transformation of precursors. Firstly, this is the only mechanism by which saturation could occur at such a low dose. No saturation was seen even at 4×10^6 Mrad electron irradiation [19] or at nearly 10^3 Mrad γ-irradiation [21] of virgin a-SiO$_2$. Secondly, the additional E_1' concentration far exceeds that which could have been produced by the other mechanisms. Pfeffer [19] finds a value of 1.8×10^{13} E_1' cm^{-2} Mrad^{-1} for electron irradiation and the corresponding value for γ-irradiation has been variously found to be 1.7×10^{15} [21], 5.5×10^{14} [22] and 1.8×10^{14} E_1' cm^{-3} Mrad^{-1} [23]. For a dose of 1.8×10^{18} O cm^{-2} the volume concentration of oxygen is so high (even at the top silicon surface it exceeds 10^{20} O cm^{-2} [8]) that it is a good approximation to assume that it is all precipitated and if it is further assumed to be present as SiO$_2$ we obtain a total SiO$_2$ volume of 4.1×10^{-5} cm^3/cm^2 of implanted surface. Hence for 7 Mrad electron irradiation the additional E_1' areal concentration would only be 5.2×10^9 cm^{-2} and only 3.5×10^{11} cm^{-2} for 5 Mrad γ-irradiation (using the largest of the creation rates previously given). These values are much less than the 5.8×10^{13} E_1' cm^{-2} actually observed.

To determine whether the precursors being transformed are indeed in the buried oxide layer or whether they are in the oxide precipitates or both we measured the increase in E_1' concentration, after a 7 Mrad electron irradiation, as a function of the oxygen dose. The results in figure 2 show that such an increase only occurs in samples which have a continuous buried oxide layer. This very strongly suggests that the E_1' centres which are reactivated by the electron or γ-radiation exist only in the buried layer whereas those present before such irradiation are only in oxide precipitates. This

in turn implies that the E'_1 centres in the two locations have different anneal behaviour but, before presenting further evidence for this, we briefly digress to estimate the volume concentration of these centres.

Figure 2 shows that the *reactivated* E'_1 areal concentration amounts to 5.8 and 10.2×10^{13} E'_1 cm^{-2} for samples with doses of 1.8 and 2.2×10^{18} O cm^{-2} and a buried a-SiO$_2$ layer of thickness 0.28 and 0.41 μm respectively. If these reactivated E'_1 centres are confined to the buried a-SiO$_2$ layer then their average volume concentration is 2.1 and 2.5×10^{18} cm^{-3} respectively. The similarity of these values suggests that the level of damage in the buried layer is independent of its thickness. These values are not much smaller than the maximum value of about 1.5×10^{19} E'_1 cm^{-3} produced by ion-implanting a-SiO$_2$ at room temperature [14].

It is also interesting to compare the volume concentration of E'_1 centres in the buried layer with that for the precipitates. If we assume as before that all the oxygen is present as SiO$_2$ we find that, for an oxygen dose $\phi = (0.75, 0.80, 0.95, 1.2, 1.4, 1.8$ (using O$_2^+$), 1.8 (using O$^+$), and 2.2) $\times 10^{18}$ O cm^{-2}, the total precipitate volume per cm^2 of implanted surface (excluding any buried layer) is (1.7, 1.8, 2.2, 2.7, 3.2, 1.3, 1.3 and 0.9) $\times 10^{-5}$ cm^3. If the E'_1 centres present before the electron γ-irradiation are only in these precipitates then their average concentration within the precipitates is (1.5, 3.9, 6.6, 7.4, 7.2, 4.7, 3.9 and 1.7) $\times 10^{18}$cm^3. These are of the same order of magnitude as for the buried layer but the average concentration clearly depends on oxygen dose with a maximum at $\phi \approx \phi_c$.

4.3. Annealing behaviour of E'_1 centres

The results of the previous section strongly suggest that E'_1 centres in the oxide precipitates and in the buried oxide layer have different annealing behaviours and the main aim of the experiments reported in this section is to record this behaviour and to see if a difference exists. We begin by describing the anneal behaviour of E'_1 centres in samples in the as-implanted state and then in section 4.3.2 present results which reveal the differences between the anneal behaviour of E'_1 centres in the two locations. The determination of activation energies is given in 4.3.3 and finally in 4.3.4 we briefly describe the room temperature annealing in these centres.

4.3.1. E'_1 centres in samples in the as-implanted state.
For the reasons given earlier we believe that these E'_1 centres are only located in the oxide precipitates even when a buried layer exists. We have already made step-annealing measurements in which the same sample is heated for 10 min intervals at successively higher temperatures with a quench to room temperature after each interval to record the EPR spectrum. We found [4] that, for samples implanted with 1.4×10^{18} O$^+$ cm^{-2} at 250, 450 or 600 °C, the E'_1 centres begin to anneal for $T \gtrsim 450$ °C. We now observe the same behaviour in a sample implanted with 1.2×10^{18} O$^+$ cm^{-2} at 620 °C. However, for a dose of 1.8×10^{18} O$^+$ cm^{-2} the annealing begins at $T \gtrsim 350$ °C [3]. One question that arises is whether or not this annealing is irreversible. To find the answer we irradiated with a small dose (≈ 14 Mrad) of electrons a sample implanted at 620 °C with 1.2×10^{18} O$^+$ cm^{-2} in which the E'_1 population had been reduced to one-half its initial value by annealing it briefly at 550 °C; the irradiation produced no detectable increase in the E'_1 signal which shows that the annealing is irreversible. More indirect evidence for the same conclusion may be drawn from figure 2 which shows that electron irradiation does not regenerate E'_1 centres in samples implanted with dose $\phi < \phi_c$ even though the

implantation temperature was high enough for E'_1 annealing to take place during the ion implantation, along with E'_1 production.

4.3.2. Irradiation–anneal–irradiation sequence.

These experiments, which reveal the difference in the annealing behaviour of reactivated E'_1 centres and those in the as-implanted samples, consist of an irradiation–anneal–irradiation sequence performed on samples implanted with 1.2×10^{18} O^+ cm^{-2} using either $^{16}O^+$ or $^{32}O_2^+$ at an implantation temperature of 560 °C. Each irradiation, at room temperature, consisted of a dose of about 10 Mrad of 30 keV electrons and each anneal was for 10 min in air at successively higher temperatures from room temperature up to 700 °C in steps of about 25 °C. After each irradiation and after each anneal the EPR spectrum of the sample was measured at room temperature. Figure 3 shows how the E'_1 areal concentration $N(E'_1)$, expressed relative to its value in the initial as-implanted sample, varies through the sequence. The behaviour observed is the same for each sample and so no distinction is made between their data points. The point marked by a full triangle refers to the $N(E'_1)$ value in the initial as-implanted state and, as we have suggested earlier, this corresponds to the E'_1 centres in the oxide precipitates. The open triangles vertically above this indicate how the total E'_1 population increases as a result of the electron radiation and the increase, we suggest, represents the E'_1 centres reactivated in the buried oxide layer. The figure shows that a measurable fall in $N(E'_1)$ after a 10 min anneal is first observed at about 100 °C. This fall must be in the reactivated E'_1 population since we have shown that the E'_1 centres in the as-implanted state of these samples do not begin to anneal until the anneal temperature is equal to or greater than 350 °C. However, this anneal at 100 °C of reactivated E'_1 centres is reversible as the figure shows that electron irradiation restores $N(E'_1)$ to its value after the very first irradiation. Raising the anneal temperature above 100 °C increases the annealing rate and this is reflected in the larger falls in $N(E'_1)$. However, in the temperature range of about 200–350 °C the $N(E'_1)$ value after annealing remains *constant* at the value corresponding to the initial as-implanted state. This is consistent with the view that annealing in this temperature range only removes the reactivated E'_1 centres leaving the E'_1 centres in the as-implanted state which do not anneal below about 350 °C in these samples. The $N(E'_1)$ value after irradiation also remains constant throughout this temperature range and this shows that up to about 350 °C the annealing of the reactivated E'_1 centres is completely reversible. Above about 350 °C there is a fall in both the $N(E'_1)$ value after annealing and in the subsequent increase in $N(E'_1)$ after irradiation. The former reflects the irreversible drop in the E'_1 centre population in the as-implanted state and the latter shows that the reactivated E'_1 centres also begin to anneal irreversibly at about the same temperature.

In summary, all the results presented so far can be explained by assuming that the E'_1 centres in the as-implanted state only exist in the oxide precipitates, that precursors remain in the a-SiO_2 buried layer which can be converted to E'_1 centres by ionizing radiation, that E'_1 centres in both regions anneal irreversibly at $T \gtrsim 350$ °C (for $\phi = 1.8 \times 10^{18}$ O cm^{-2}) and that only those centres in the buried layer exhibit reversible annealing up to about 350 °C.

The annealing measurements reported so far, which entailed the heating of one or two samples at successively higher temperatures, do not yield a value for the activation energy. To obtain this, isochronal measurements were made and these are reported in the next section.
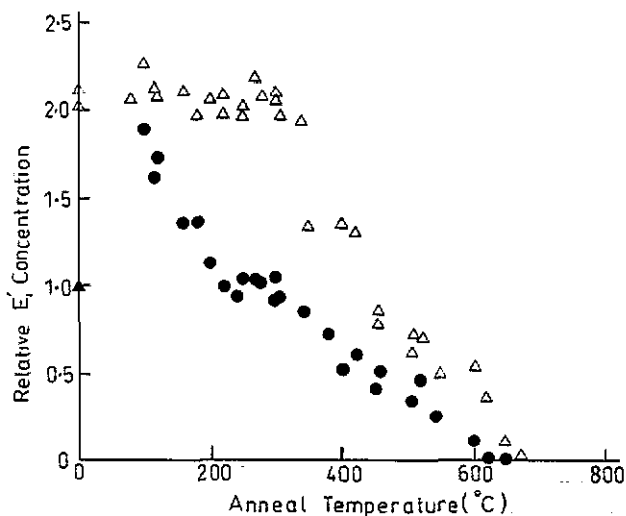
Figure 3. The relative E' centre concentration dependence on anneal temperature. The concentration is measured after each electron irradiation (open triangles) and subsequent anneal (full circles) and its value relative to that in the initial unirradiated, unannealed state is plotted.

4.3.3. Isochronal annealing. Despite the scarcity of samples we obtained a set which were all implanted with 1.8×10^{18} cm^{-2} of 200 keV ^{16}O at $T_i = 580\,^\circ$C. Most of these were annealed for 10 min in nitrogen at different temperatures. For each sample the E'$_1$ areal concentration was measured before (N_1) and after (N_2) annealing and also after (N_3) annealing plus an irradiation dose sufficiently large to transform all E'$_1$ centre precursors into E'$_1$ centres. The ratio of N_2/N_1 as a function of temperature corresponds to the (irreversible) annealing curve for E'$_1$ centres in the precipitates. The concentration of reactivated E' centres in the buried layer, after annealing, is $(N_3 - N_2)$. The corresponding value before annealing could not be measured directly but could be calculated using the value of N_1 and the fact that unannealed samples from the set, *not* used in the isochronal measurements, were always found to have a population ratio N (reactivated E'$_1$)/$N_1 = 2.1 \pm 0.1$. Figure 4 displays the temperature dependence of the relative concentration of both reactivated E'$_1$ centres and those in the precipitates; no difference in their irreversible anneal behaviour can be seen.

In order to make a direct comparison with the results obtained for E'$_1$ centres produced in bulk amorphous SiO$_2$ by ion implantation we follow the methods used by Golanski *et al* [24] to find the activation energy for the *irreversible* isochronal annealing behaviour of these centres. They used two different models for a diffusion-limited thermal activated process: a first-order unimolecular recombination model and Simpson's and Sosin's model [25] for bimolecular recombination. The latter assumes that the recombination of the interstitial–vacancy pair (in this case both oxygen) is favoured by their proximity. Golanski *et al* [24] found that the activation energy was almost independent of the initial distribution of the distance between members of a pair whether it was Gaussian, exponential or modified exponential. With the last of these distributions, $g(r)$, for which

$$g(r) = ar \exp(-r/\lambda r_0)$$

the E_1' concentration, N, relative to its initial value, N_0, is given by [24]

$$\frac{N}{N_0} = 1 - (1 + \lambda)^{-1} \left[1 - \exp \left(\frac{\alpha}{2} \right)^2 \operatorname{erfc} \left(\frac{\alpha}{2} \right) \right]$$

where a is a normalization constant, r_0 is the radius of a sphere, centred on the vacancy site, in which the interstitial is captured by the vacancy, $\alpha = \sqrt{4Dt}/\lambda r_0$ and the diffusion coefficient for interstitial migration is $D = D_0 \exp(-E_a/kT)$.

For the first-order process of unimolecular recombination the decrease in E_1' concentration is given by

$$\frac{N}{N_0} = \exp(-kt)$$

where the first-order rate constant $k = k_0 \exp(-E_a/kT)$.

Golanski *et al* obtained equally good fits with both these models provided that in each case a Gaussian distribution of E_a values was included. They assumed that $k_0 = 10^{13}$ s^{-1}, $r_0 = 5$ Å, $D_0 = 10^{-3}$ cm^2 s^{-1} and obtained $E_a = 2.9$ eV, $\sigma(E_a) = 0.35$ eV with the unimolecular model and $E_a = 2.9$ eV, $\sigma(E_a) = 0.25$ eV, $\lambda = 0.1$ with the other model; these values are for E_1' centres produced by O^+ implantation and differ slightly from those for such centres produced by He$^+$, Bi$^+$ and N$^+$ implantation [24].
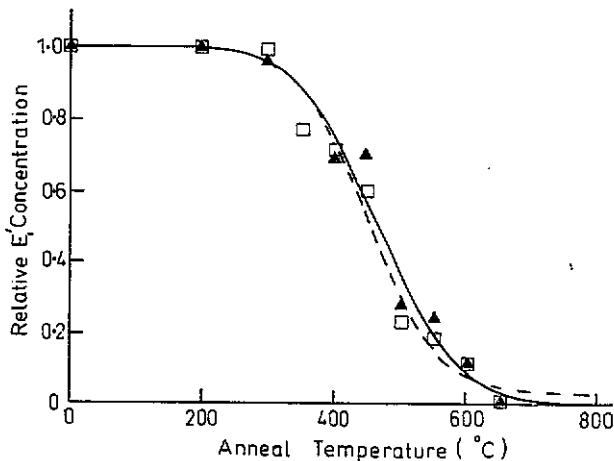

Figure 4. Irreversible isochronal anneal of the E_1' centres in the precipitates (open squares) and those reactivated in the buried layer (full triangles). Each anneal is for 10 min in flowing nitrogen. The best fits obtained using the unimolecular model and the Simpson and Sosin model are shown by the full and broken lines respectively; the parameters are given in the text.

Figure 4 shows that our data too fit equally well with both models provided that a Gaussian distribution of E_a values is included. Using the previously given values for k_0, r_0 and D_0 we find $E_a = 2.35$ eV, $\sigma(E_a) = 0.3$ eV for the unimolecular model and $E_a = 2.45$ eV, $\sigma(E_a) = 0.25$ eV, $\lambda = 0.05$ for the other model. The small value of λ is required to fit the tail of the annealing curve. Golanski *et al* [24] pointed out that $\lambda = 0.1$ implies that 99% of the interstitial oxygen atoms available for the recombination

process lie within 7.5 Å of the vacancy site and that under these conditions the Simpson and Sosin model converges towards a first-order process.

It must be noted that the values of E_a are not unique as they depend on the choice of k_0 and D_0. Devine and Fiori [26] obtained a good fit to the isochronal annealing of reactivated E'_1 centres in Ar^+ implanted thermal SiO_2 using first-order kinetics with $E_a = 2.3$ eV, $\sigma(E_a) = 0.26$ eV and $k_0 = 2 \times 10^{11}$ s^{-1}. For $k_0 = 10^{11}$ s^{-1} we find $E_a = 2.15$ eV, $\sigma(E_a) = 0.3$ eV.

4.3.4. E′ annealing at room temperature. Preliminary measurements indicate that the E'_1 centres reactivated by electron or γ-irradiation anneal at room temperature with an approximate $\log t$ time dependence and that after 1 week their population has dropped to about 70% of that which exists 1 h after the irradiation ceases.

We have not detected any room temperature annealing of the E'_1 centres in the as-implanted state of the samples.
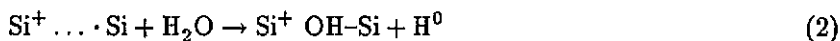
5. Identity of E′ centres

Many varieties of E′ centres have been identified. Apart from the ones in quartz those in a-SiO$_2$ include E'_α, E'_β, E'_γ [27], E'_δ [28], E'_f [29] which is claimed to be possibly unique to thin films of a-SiO$_2$ and E'_s [30] which is suggested to be at the surface of SiO$_2$. These have slightly different principal g values but almost the same average value $\bar{g} = \frac{1}{3}(g_1 + g_2 + g_3)$ which, with the exception of E'_δ with $\bar{g} = 2.0020$, is in the range 2.0007 to 2.0010. The line we observe for both as-implanted samples and those subsequently irradiated is too broad and nearly symmetric—as is characteristic of E'_1 centres produced by high-dose ion implantation [17]—to allow us to eliminate any of these except E'_δ on the basis of shape and position alone. However, E'_α—at least in low-OH silicas—and E'_β begin to bleach rapidly at 200 and 250 K respectively [27] and so are unlikely to be present. Of the remaining types by far the most likely candidate—at least for the E′ centres in the buried SiO$_2$ layer—is the E'_γ centre (or E'_1 centre with which it is structurally equivalent [31]). The E'_1 centre has been shown [1] to be a bridging oxygen vacancy with a hole trapped primarily on one of the silicon atoms nearest the vacancy and an unpaired spin on the other; it may be represented as $\equiv Si^+ \ldots \cdot Si \equiv$. This is the type of E′ centre produced by the room-temperature implantation of a variety of ions into thermally grown SiO$_2$ [14, 15]. Its spectrum has a zero crossing g value of 2.0002 ± 0.0005 and at sufficiently high doses becomes almost symmetric [14, 17]. When created by ion implantation it is found to begin to anneal at about 100 °C [15, 17] but for temperatures less than or equal to 300 °C it can be reactivated by ionizing radiation and it only anneals irreversibly for temperatures greater than or equal to 500 °C [15, 18, 24, 26]. The E′ centres in the buried SiO$_2$ layer have very similar characteristics and we believe therefore that they too are E'_1 centres. The only way in which the E′ centres in the precipitates differ from those in the buried layer is that they exhibit no low temperature reversible annealing; it seems plausible that they are also E'_1 centres in which case this difference must reflect their different locations and should give a clue to the nature of the anneal mechanisms.

6. E′$_1$ anneal mechanism

Several ways in which E'_1 centre annealing occurs have been proposed including

$$Si^+ \ldots \cdot Si + O_2 \rightarrow Si \cdot O\text{-}O\text{-}Si \tag{1}$$

$$\text{Si}^+ \ldots \cdot \text{Si} + \text{H}_2\text{O} \rightarrow \text{Si}^+ \text{ OH--Si} + \text{H}^0 \qquad (2)$$

$$\text{Si}^+ \ldots \cdot \text{Si} + e^- \rightarrow \text{Si} \cdot \ \cdot \text{Si} \qquad (3)$$

(1) was proposed by Edwards and Fowler [32] and the growth of the superoxide radical Si–O–O · accompanying the decay at $T \gtrsim 100\,°\text{C}$ of E'_1 centres in bulk low-OH silicas [33–35] together with the results of Pfeffer [35] for degassed and oxygen stuffed low-OH silicas strongly support the occurrence of this reaction in these silicas. For high-OH silica the E'_1 annealing only begins at $T \gtrsim 260\,°\text{C}$ and is assumed to occur by the second process [36]. E'_1 centres have been identified [2] as the source of trapped positive charge in the oxide of MOS structures and the annealing of this charge has been extensively studied. Often the charge is mostly located within 10 nm or so of the Si/SiO₂ interface [2, 37] and many authors [37–41] have attributed its anneal to reaction 3 with the electron tunnelling from the silicon to the trapped charge. Some [42] find the annealing of this charge to be independent of temperature between 25 and 125 °C while others [39, 43] find that its rate increases continuously throughout this range. As well as its removal by tunnelling processes, several measurements [44–46] of thermally stimulated current in MOS devices suggest that the trapped holes can be excited to the SiO₂ valence band with activation energies in the range of about 0.8 to 1.6 eV.

The first question that now arises is which, if any, of these mechanisms is responsible for the E'_1 annealing at $100\,°\text{C} \lesssim T \lesssim 350\,°\text{C}$ which as previously shown is reversible but only occurs for E'_1 centres in the buried layer. Its onset at about 100 °C is consistent with the first mechanism. The fact that we detected no superoxide radical resonance is not surprising since it is much broader and hence, for a given number of spins, has a much smaller peak-to-peak height than the E'_1 centre resonance. There certainly would be O₂ molecules available in the buried layer since the layer grows by the diffusion towards its interfaces of the excess oxygen implanted mainly at its centre. On the other hand many of the precipitates may be deficient in oxygen—there is evidence [9] that SiO$_x$, $x < 2$ is present—and therefore the oxygen required for the removal of the E'_1 centres in these precipitates would presumably have to diffuse through the surrounding silicon to reach the oxygen vacancy. This may account for the absence of E'_1 annealing in the precipitates for $T \lesssim 350\,°\text{C}$ since the activation energy for the diffusion of O₂ in silicon is in the range 2.4–3.5 eV [47] which is much higher than the range 0.85–1.26 eV for O₂ in SiO₂ [32]. For (1) to be the mechanism responsible it must be reversible; unfortunately it is not known at present if this is the case. Mechanism (2) may be ruled out because it only begins for $T \lesssim 260\,°\text{C}$ but mechanism (3) is a possibility. It is certainly likely to be reversible. Robertson [48] has pointed out that the neutral oxygen vacancy is a precursor of the E'_1 centre and can therefore act as a hole trap. It seems reasonable that, as in the MOS devices, E'_1 centres close to the oxide precipitate/silicon interface are removed through recombination of the trapped holes with electrons tunnelling into the precipitates from the silicon. A tunnelling front is believed to move logarithmically with time into the SiO₂ and it has been estimated [38] that after 1 week the trapped positive charge within a layer of thickness 5 nm is removed. There is some evidence that this occurs in the precipitates. It was shown in section 4.2 that the average E'_1 concentration within the precipitates is a maximum for an oxygen dose $\approx \phi_c$. This could be because in our EPR samples, which were implanted several months prior to the EPR measurements, the tunnelling electrons have removed E'_1 from the outer shell, a few nanometres thick, of the precipitates leaving only those further inside. As the oxygen concentration is

increased by increasing the dose the precipitates grow; the proportion of SiO_2 not contained within this shell will therefore increase and so the overall average volume concentration of E'_1 centres in the precipitates will also increase. However, once ϕ exceeds ϕ_c the formation of the buried layer, consuming as it does the largest precipitates which are at the peak of the plot of the oxygen against depth distribution, will decrease this proportion and hence the average E'_1 concentration should also decrease as is observed.

The absence of E'_1 centres in the outer shell of the precipitates also explains the change produced by etching the sample. The silicon removed first contains the smallest precipitates; these, having a high surface/volume ratio, may have a significant proportion of all the P_b centres at the oxide precipitate/silicon interface but a small proportion of the E'_1 centres and hence the etch would initially decrease the P_b centre population more than that of the E'_1 centres, as we observed [3].

One result which casts doubt on the idea of an outer shell devoid of E'_1 centres is the absence of any increase in the E'_1 population after samples, without a buried layer, are subsequently irradiated with electrons or γ-rays; this should regenerate the E'_1 centres within the shell.

Whether or not the E'_1 centres are removed from this outer shell by electrons tunnelling from the silicon at room temperature there remains the question of whether mechanism (3) can explain the anneal behaviour in the range $100 \lesssim T \lesssim 350\,°C$. The E'_1 centres must be more or less uniformly distributed throughout the buried layer and hence the great majority are too far from the Si/SiO_2 interface to be annealed by electrons tunnelling from the silicon. It might be supposed, however, that the electron captured by the E'_1 centre has been thermally excited from the SiO_2 valence band but we cannot see why annealing by this process should happen in the buried layer but not in the precipitates and consequently we believe that this is not the dominant mechanism.

We now briefly consider what mechanism is responsible for the irreversible annealing at $T \lesssim 350\,°$, with $E_a \approx 2.4$ eV, of the E'_1 centres in both the buried layer and the precipitates. The irreversibility suggests that reformation of the Si–O–Si network occurs and if mechanism (1) is responsible for the reversible annealing stage then such reformation entails the dissociation of the peroxy radical. Such a process has already been suggested [18, 26] and the fact that the temperature dependence of the irreversible annealing of E'_1 centres in thermally grown a-SiO_2 matches that of peroxy radicals in suprasil W1 [26] supports this suggestion. This process is different from the Simpson and Sosin model oxygen interstitial–oxygen vacancy recombination used by Golanski *et al* [24] but the value of E_a, which does not appear to be strongly model-dependent, is likely to be about right. It is not clear why this value is less than that obtained by them for E'_1 centres in ion-implanted thermally grown SiO_2. As regards the E'_1 centres in the precipitates their irreversible anneal takes place with an activation energy (≈ 2.4 eV) very close to that (2.4–3.5 eV) expected for their reversible conversion to peroxy radicals. The peroxy radical formation and its dissociation may therefore occur in the precipitates at almost the same temperature so that no reversible stage is seen.

Since the implantation temperature exceeds that at which the E'_1 centres begin to anneal irreversibly it might be thought surprising that any E'_1 centres are found at all in the as-implanted samples but the ion implantation also creates new centres at the same time. The fact that, as shown in section 4.2, the average volume concentration of the reactivated centres in the buried layer is about seven times less than the maximum

produced by ion implanting a-SiO_2 at room temperature surely reflects the presence of this competing anneal process during implantation.

Finally, we briefly consider the mechanism for the room temperature anneal which we only observe for the reactivated E_1' centres in the buried layer. Positive charge trapped close to the Si/SiO_2 interface of MOS devices certainly does anneal at room temperature. It is thought to do so by the electron tunnelling process previously mentioned but as the buried oxide layer is either 0.28 or 0.41 μm thick and the centres must be nearly uniformly distributed throughout the layer, most must be too far from the interfaces to be removed by this process. It may be that those which anneal at room temperature do so by some strain-related athermal process or else they are not E_1' centres at all but some other less stable variant such as E_α' [27]. We intend to investigate this further.

7. Conclusions

Silicon wafers which have been implanted at about 500–600 °C with approximately 10^{18} O cm^{-2} only contain E_1' centres in the oxide precipitates. However, E_1' precursors remain in the buried oxide layer and can be converted to E_1' centres by electron or γ-irradiation. These results reflect the different anneal behaviour of these centres in the two locations. In both they exhibit irreversible annealing which, for samples implanted with 1.8×10^{18} O cm^{-2} at 200 keV, begins at about 350 °C. However, only those in the buried layer anneal reversibly below this temperature. We suggest that the most likely dominant mechanism of the reversible annealing, at least in the temperature range 100–350 °C, is the capture of O_2 by the E_1' centre to form a peroxy radical, rather than the capture of an electron to form a neutral oxygen vacancy. We suggest that this reversible process is not seen for E_1' in the oxygen-deficient precipitates because its occurrence there requires the diffusion of O_2 through the surrounding silicon and the activation energy for this is close to that of about 2.4 eV at which the irreversible anneal, which may be associated with peroxy radical dissociation and Si–O–Si network reformation, of the E_1' centres occurs.

There is some indirect evidence that the E_1' centres in the outer layer of the precipitates are removed by the capture of electrons tunnelling from the silicon.

References

[1] Feigl F J, Fowler W B and Yip K L 1974 *Solid State Commun.* **14** 225
[2] Lenahan P M and Dressendorfer P V 1984 *J. Appl. Phys.* **55** 3495
[3] Barklie R C, Hobbs A, Hemment P L F and Reeson K 1986 *J. Phys. C: Solid State Phys.* **19** 6417

[4]   Barklie R C, Ennis T J, Hemment P L F and Reeson K 1988 *Nucl. Instrum. and Meth.* B 32
      433
[5]   Taylor M R, Tuppen C G, Arrowsmith R P, Dobson R M, Glaccum A E, Wilson M C, Booker
      G R and Hemment P L F 1983 *Microscopy of Semiconducting Materials (Inst. Phys. Conf.
      Ser. 67)* (Bristol: Institute of Physics) p 485
[6]   Reeson K, Marsh C D, Chater R J, Kilner J A, Robinson A K, Christensen K N, Hemment P L
      F, Harbeke G, Steigmeier E F, Booker G R and Celler G K 1988 *Microelectronic Engineering*
      8 163
[7]   Kilner J A, Littlewood S, Hemment P L F, Maydell-Ondrusz E and Stephens K G 1983 *Nucl.
      Instrum. and Meth.* 218 573
[8]   Hemment P L F, Maydell-Ondrusz E, Stephens K G, Butcher J, Ioannou D and Alderman J
      1983 *Nucl. Instrum. and Meth.* 209/210 157
[9]   Harbeke G, Steigmeier E F, Hemment P L F, Reeson K J and Jastrzebski L 1987 *Semicond.
      Sci. and Tech.* 2 687
[10] Holland O W, Sjoreen T P, Fathy D and Narayan 1984 *Appl. Phys. Lett.* 45 1081
[11] Jaussaud C, Stoemenos J, Margill J, Dupuy M, Blanchard B and Bruel M 1985 *Appl. Phys.
      Lett.* 46 1064
[12] Sjoreen T P, Holland O W, Fathy D, More K and Davis R F 1985 *Nucl. Instrum. and Meth.* B
      10/11 574
[13] Krause S J, Jung C O, Lorigan R P and Burnham M E 1986 *Mat. Res. Soc. Symp. Proc. 53*
      257 (Materials Research Association)
[14] Devine R A B and Golanski A 1983 *J. Appl. Phys.* 54 3833
[15] Golanski A, Devine R A B and Oberlin J C 1984 *J. Appl. Phys.* 56 1572
[16] Devine R A B and Golanski A 1984 *J. Appl. Phys.* 55 2738
[17] Devine R A B 1984 *Nucl. Instrum. and Meth.* B 1 378
[18] Devine R A B 1984 *J. Appl. Phys.* 56 563
[19] Pfeffer R L 1985 *J. Appl. Phys.* 57 5176
[20] Van Lint V A, Flanagan T M, Leadon R E, Naber J A and Rogers, V C 1980 *Mechanisms of
      Radiation Effects in Electronic Materials* vol 1 (New York: Wiley) p 44
[21] Griscom D L, Friebele E J, Long K T and Fleming J W 1983 *J. Appl. Phys.* 54 3743
[22] Dooryhee E, Langevin Y, Borg J, Duraud J P and Balanzat E 1988 *J. Appl. Phys.* 63 1399
[23] Marquardt C L and Sigel Jr G H 1975 *IEEE Trans. Nucl. Sci.* 22 2234
[24] Golanski A, Pfister J C and Nicolle T 1986 *J. Appl. Phys.* 59 1096
[25] Simpson H M and Sosin A 1970 *Rad. Effects* 3 1
[26] Devine R A B and Fiori C 1985 *J. Appl. Phys.* 58 3368
[27] Griscom D L 1984 *Nucl. Instrum. and Meth.* B 1 481
[28] Griscom D L and Friebele E J 1986 *Phys. Rev.* B 34 7524
[29] Carlos W E 1986 *Appl. Phys. Lett.* 49 1767
[30] Hochstrasser G and Antonini J F 1972 *Appl. Surf. Sci.* 32 644
[31] Griscom D L, Friebele E J and Sigel Jr G H 1974 *Solid State Commun.* 15 479
[32] Edwards A H and Fowler W B 1982 *Phys. Rev.* B 26 6649
[33] Stapelbroek M, Griscom D L, Friebele E J and Sigel Jr G H 1979 *J. Non-Cryst. Solids* 32 313
[34] Devine R A B 1987 *Phys. Rev.* B 35 9783
[35] Pfeffer R L 1988 *The Physics and Technology of Amorphous SiO2* ed R A B Devine (New
      York: Plenum) p 181
[36] Griscom D L 1986 *Structure and Bonding in Noncrystalline Solids* ed G E Walrafen and A G
      Revesz (New York: Plenum) p 369
[37] Oldham T R, Lelis A J and McLean F B 1986 *IEEE Trans. Nucl. Sci.* 33 1203
[38] Saks N S, Ancona M G and Modolo J A 1989 *IEEE Trans. Nucl. Sci.* 31 1249
[39] Schwank J R, Winokur P S, McWhorter P J, Sexton F W, Dressendorfer D V and Turpin D C
      1984 *IEEE Trans. Nucl. Sci.* 31 1434
[40] Benedetto J M, Boesch H E, McLean F B and Mize J P 1985 *IEEE Trans. Nucl. Sci.* 32 3916
[41] Lelis A J, Boesch H E, Oldham T R and McLean F B 1988 *IEEE Trans. Nucl. Sci.* 35 1186
[42] Lelis A J, Oldham T R, Boesch H E and McLean F B 1989 *IEEE Trans. Nucl. Sci.* 36 1808
[43] Lakshmanna V and Vengurlekar A S 1988 *J. Appl. Phys.* 63 4548
[44] Shanfield Z 1983 *IEEE Trans. Nucl. Sci.* 30 4064
[45] Shanfield Z 1984 *IEEE Trans. Nucl. Sci.* 31 1242
[46] Shanfield Z and Moriwaki M M 1985 *IEEE Trans. Nucl. Sci.* 32 3929

[47] Wilkes J 1988 *Properties of Silicon, EMIS Data Reviews Series No 4* (London: INSPEC) p 281

[48] Robertson J 1988 *The Physics and Technology of Amorphous SiO_2* ed R A B Devine (New York: Plenum) p 91